Solid Freeform Fabrication 2016: Proceedings of the 27th Annual International Solid Freeform Fabrication Symposium – An Additive Manufacturing Conference
Reviewed Paper

EFFECT OF BUILD ORIENTATION ON THE FATIGUE BEHAVIOR OF STAINLESS STEEL 316L MANUFACTURED VIA A LASER-POWDER BED FUSION PROCESS

Rakish Shrestha[1], Jutima Simsiriwong[1], Nima Shamsaei[2,*], Scott M. Thompson[2], Linkan Bian[3]

[1]Center for Advanced Vehicular Systems (CAVS), Mississippi State University, MS 39762

[2]Department of Mechanical Engineering, Auburn University, Auburn, AL 36849

[3]Department of Industrial and Systems Engineering, Mississippi State University, MS 39762

*Corresponding author: shamsaei@auburn.edu

Abstract

In this study, the effects of build orientation on the mechanical properties and fatigue life of stainless steel (SS) 316L, fabricated using the Laser-Powder Bed Fusion (L-PBF) additive manufacturing (AM) process, were investigated under monotonic tensile and uniaxial strain-controlled fully-reversed (R_ε = -1) cyclic loadings. Tensile tests were conducted at a strain rate of 0.001 s^{-1}, while fatigue tests were performed at strain amplitudes ranging from 0.1% to 0.4% at various frequencies to have a nearly consistent average strain rate in all tests. The comparison between the tensile properties of additively manufactured and wrought SS 316L revealed that L-PBF specimens exhibited higher yield and ultimate tensile stresses as compared to the wrought specimen. In addition, the elongation to failure of the wrought specimen was similar to that of the horizontally oriented specimen, while it was lower relative to specimens built in vertical and diagonal directions. From the strain-life fatigue analysis, the diagonally oriented L-PBF specimens generally exhibited lower fatigue strength as compared to vertical and horizontal specimens. The fractography analysis revealed three major types of defects to be responsible for the crack initiation and failure. These included (1) voids formed due to lack of fusion between the subsequent layers and entrapped gas, (2) inclusions formed due to the partially melted powder particles, and (3) un-melted powder particles clustered near a void.

Keywords: Fatigue, Tensile properties, Fractography, Build orientation, Additive manufacturing

1. Introduction

Additive manufacturing (AM) processes are gaining attention in both industrial and the academic sectors due to their unique ability to fabricate parts by joining materials layer by layer as opposed to the traditional subtractive fabrication process. As a result, AM processes provide an advantage to produce parts with complex geometry and parts with lower number of assemblies. In general, there are two types of laser-based additive manufacturing techniques for fabricating metallic parts, which are the Laser-Powder Bed Fusion (L-PBF) and the Direct Laser Deposition (DLD) (or Directed Energy Deposition - Laser) processes. In the L-PBF technique, a thin layer of

metallic powder is first deposited on a build plate, which is also known as a substrate. A high intensity laser moving in a pre-defined pattern melts the powder, forming a micro-sized melt pool, which rapidly solidifies once the laser is removed. The solidification process leads to the formation of a solid layer of metal, and this process is repeated for each layer until the entire part is completed. Since the build process involves very high temperatures, the entire process is conducted in an inert environment to minimize oxidation of the fabricated parts.

One of the major drawbacks of using the AM process is the susceptibility of its parts to defects, such as inclusions that are formed due to un-melted powder particles, and voids that are created by the lack of fusion (LOF) between the subsequent layers and entrapped gas [1, 2]. Formation of such defects depends on the process parameters such as laser power, hatch spacing, laser pattern, layer thickness, and build orientation [3]. Hence, additively manufactured components may generally exhibit poor fatigue properties when compared to their wrought counterparts, as the defects have significant effects on the fatigue behavior of parts subjected to cyclic loading. However, such parts often demonstrate comparable or superior mechanical properties as compared to that of wrought material under tensile loading [4]. Further studies on the optimization of L-PBF process parameters are required to fabricate AM parts with better fatigue properties [3].

Although various metallic materials may be used for L-PBF, stainless steel (SS) 316L was selected in this study. This particular steel alloy is extensively used in the marine, architectural, and biomedical industries due to its excellent corrosion resistance, weldability, and dynamic stability in wide range of temperature [5]. In biomedical industries, SS 316L is primarily used in orthopedic implants for hip and knee replacements [6], as well as internal fixation of femur bones [7]. Therefore, as most of the components in the aforementioned applications are subject to cyclic loading throughout their lifetime, it is necessary to perform the fatigue evaluation on SS 316L.

Though the applications of SS 316L are popular in biomedical industries, only a small number of research has been performed on mechanical properties of additively manufactured SS 316L [8, 9] and even fewer research have been conducted on their fatigue behavior. Yadollahi et al. [4] investigated the mechanical and microstructural properties of DLD SS 316L. It was found that AM parts possessed higher yield and ultimate stresses relative to their cast and wrought forms. In addition, the elongation to failure was found to be lower for specimens fabricated using the AM process due to defects such as voids and un-melted powder. Sperings et al. [10] investigated the fatigue behavior of two different types of SS (316L and 15-5 precipitation hardening) manufactured using the L-PBF process. It was found that the fatigue life of L-PBF SS 316L has 25% lower fatigue strength at lower strain amplitudes relative to its conventional forms. Hence, further study is required on fatigue performance in order to optimize and select better process parameters for defect-minimized, fatigue resistance fabrication of additively manufactured SS 316L.

In this study, the effects of build orientation on the mechanical properties of SS 316L manufactured using the L-PBF process is investigated. First, the experimental setups for conducting tensile and fatigue tests, as well as the fractography analysis are given. The experimental results is then presented and discussed. Finally, some conclusions are made based on the experimental results.

2. Experimental Setup

Gas atomized SS 316L powder (Renishaw, Inc.), with an average particle size of 25 μm, was utilized for specimen fabrication. Using a scanning electron microscopy (SEM), it was found that the majority of the powder possessed a spherical shape and ranged from 9 to 45 μm in diameter, as shown in Fig. 1(a). The SS 316L rods, with 85 mm length and 8 mm diameter, were fabricated in an argon-purged AM machine (Renishaw AM250) in three different build directions. These are vertically-upward (V), horizontal (H), and diagonal (at an angle of 45° to the substrate (D)), as shown in Figs. 1(b)-(d), respectively. All test specimens were made using default process parameters as presented in Table 1. These process parameters, including the laser power, scanning speed, hatching pitch, and layer thickness, were provided by Renishaw Inc. Ten specimens in V and D directions and six specimens in the H direction were fabricated per build using a meander scan pattern. For specimens built in V and D directions, support structures of 5 mm were used only at the base of the cylindrical rod as shown in Figs. 1(b) and (d). Whereas, for specimens built in H direction, support structures were fabricated for every 0.5 mm along the length of the specimen, as shown in Fig. 1(c).

After fabrication, L-PBF SS 316L rods were machined using a computer numeric control lathe into round specimens with uniform gage section following the ASTM E606 standard [11] to the dimensions shown in Fig. 2. The gage sections of the machined specimens were then polished using different grit sand papers to remove machining marks and to reduce the surface roughness in the gage section to approximately 1 μm.

Both monotonic tensile and fatigue tests were conducted at room temperature using a servo hydraulic MTS 858 machine with 25 kN load cells. Axial strain was measured using a MTS mechanical extensometer. The monotonic tensile tests were conducted at a strain rate of 0.001 s^{-1}, first under the strain-controlled loading, followed by the displacement-controlled loading. Since the elongation to failure for the L-PBF SS 316L exceeded the travel distance (4 mm) of the extensometer, the tensile test was switched from strain-control to displacement-control mode to avoid damaging the extensometer. Furthermore, the uniaxial fully-reversed (R_ε = -1) strain-controlled fatigue tests were conducted under different strain amplitudes ranging from 0.1% to 0.4% following the ASTM E606 standard [11]. Test frequency for all fatigue tests was varied to maintain a nearly constant average strain rate and to eliminate the effects of strain rate on the fatigue life of investigated L-PBF SS 316L parts. The fractography analysis on the fractured surface of the specimens was conducted using a SEM to investigate failure mechanisms and to determine microstructural factors that are responsible for crack initiation.

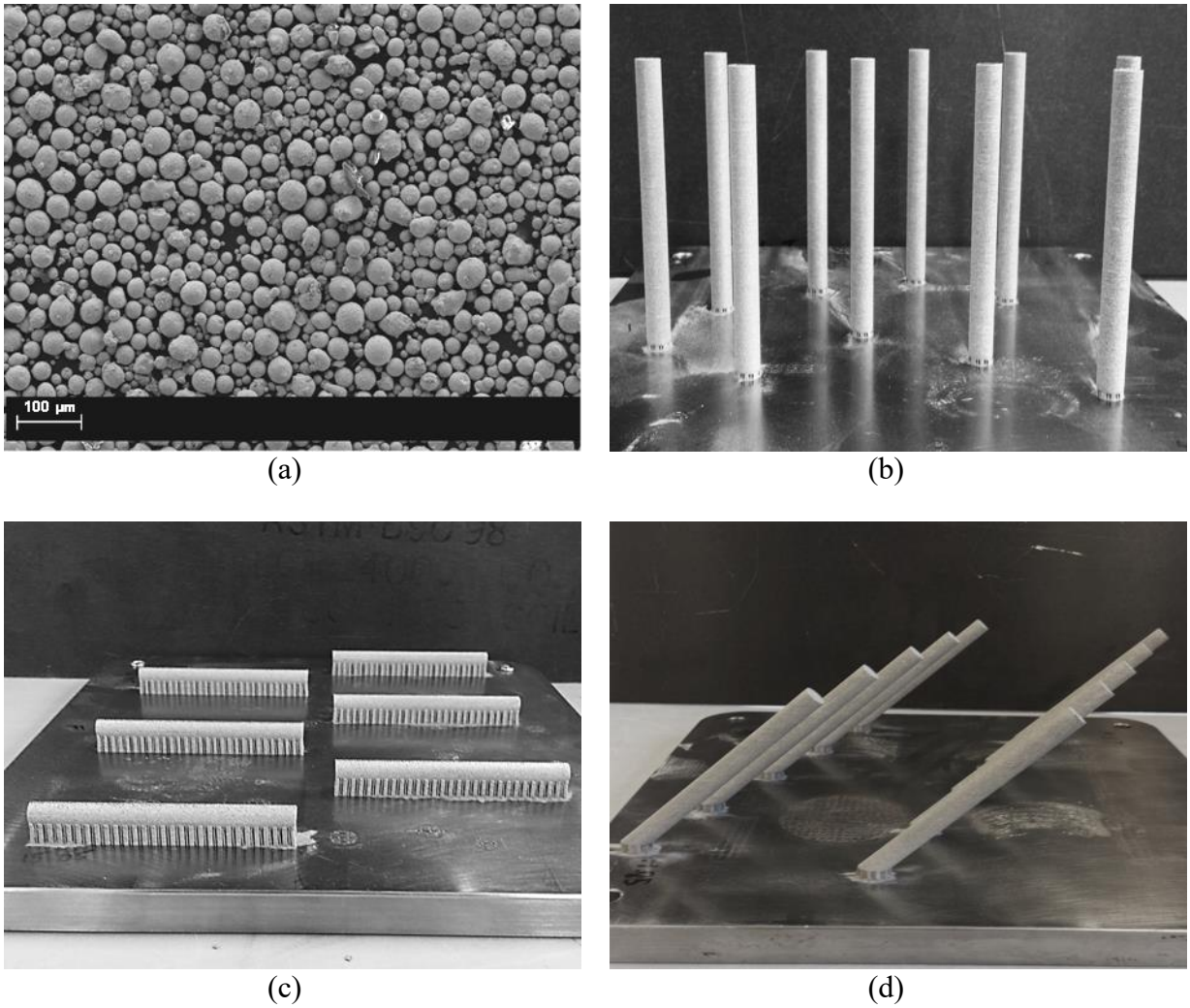

Figure 1. (a) SEM image of as-received SS 316L powder along with L-PBF SS 316L cylindrical rods (still attached to substrate) built in (b) vertical, (c) horizontal, and (d) diagonal directions.

Table 1. L-PBF process parameters used for fabricating SS 316L rods.

Laser Power (W)	Scanning Speed (m/s)	Hatching Pitch (mm)	Layer Thickness (µm)
400	1	0.1	30

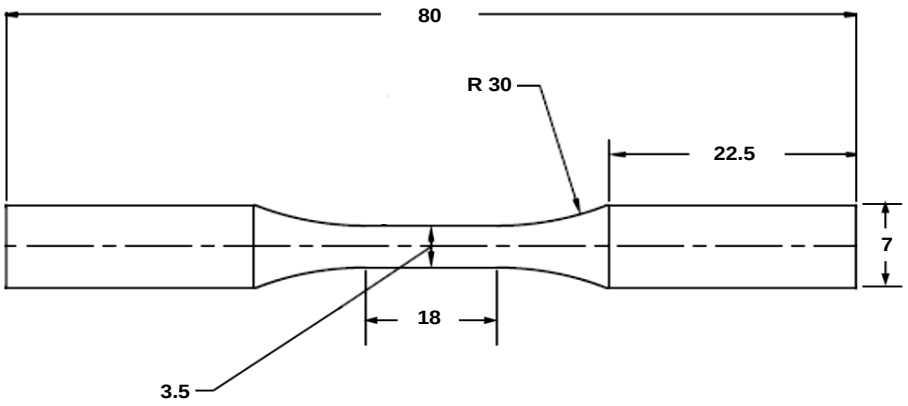

Figure 2. Specimen geometry for both monotonic tensile and fatigue tests (dimensions in mm) based on ASTM E606 standard.

3. Experimental Results and Discussions

Monotonic Behavior

The engineering stress-strain behavior inherent to the H, D, and V oriented specimens under monotonic tensile loading at a strain rate of 0.001 s^{-1} is shown in Fig. 3. The comparison of different tensile properties between the L-PBF 316L and wrought SS 316L [4,10,12] was also conducted. These values, including Young's modulus, yield stress, ultimate tensile stress, and elongation to failure, for wrought SS 316L reported in [4,10,12] are listed in Table 2. From the results, the Young's modulus for wrought specimen of 200 GPa was observed to be similar to the D specimen and higher relative to the V and H specimens. On the other hand, the yield and ultimate tensile stresses were found to be considerably higher for the investigated L-PBF SS 316L specimens as compared to those reported for wrought SS 316L [4,10]. Among the specimens built in three different directions, the vertically oriented specimen exhibited the greatest elongation to failure (~50% strain), which is approximately 25% higher than that of wrought material. This trend, where the vertically built specimens possessed a higher elongation to failure but lower yield and ultimate tensile stresses as compared to H specimens, also has been reported in [13] for additively-manufactured SS 316L.

The SEM images displaying an overall fractured surface for the H, D, and V specimens that failed under monotonic tensile loading are shown in Fig. 4(a)-(c), respectively. It can be noticed that the gage section of the V specimen, exhibiting the highest elongation to failure, deformed from a circular to an ellipse shape (Fig. 4(c)), while such deformation was not as prominent in specimens fabricated in H (Fig. 4(a)) and D (Fig. 4(b)) directions. Voids due to process-laden gas entrapment and LOF between layers, as shown in Fig. 4, were observed on the facture surfaces of all tensile specimens irrespective to the build orientation.

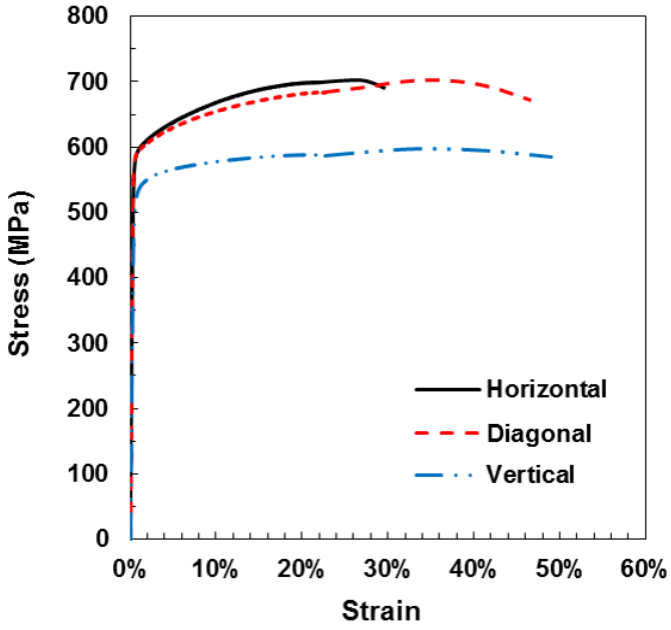

Figure 3. Monotonic tensile engineering stress-strain curves for L-PBF SS 316L specimens built in horizontal (H), diagonal (D), and vertical (V) directions.

Table 2. Tensile properties of wrought SS 316L [4,10,12].

Yield Stress (MPa)	Ultimate Tensile Stress (MPa)	Young's Modulus (GPa)	Elongation (%)
255-310	535-623	200	30-40

As illustrated in Fig. 3, the elongation to failure was lowest for the horizontally built specimen, while it was comparable for the D and V specimens. Un-melted powder particles were evident on these fracture surfaces, especially for vertically built specimens. However, these defects apparently did not affect the monotonic tensile behavior of L-PBF SS 316L. The relatively lower elongation to failure observed for H specimens may be related to the longer inter-layer time interval, which resulted in higher cooling rate in these specimens as compared to V and D specimens. This higher cooling rate can in turn lead to finer microstructure in H specimens [4, 12]. Moreover, higher yield and ultimate tensile stresses observed for L-PBF SS 316L specimens (in all three conditions) as compared to the wrought counterpart can be related to the fine microstructure resulting from fast cooling rate during AM fabrication [3, 4, 10, 14]. Further studies on the microstructure, defect statistics, and phase transformation are required to thoroughly understand the effects of build orientation on the tensile behavior of L-PBF SS 316L.

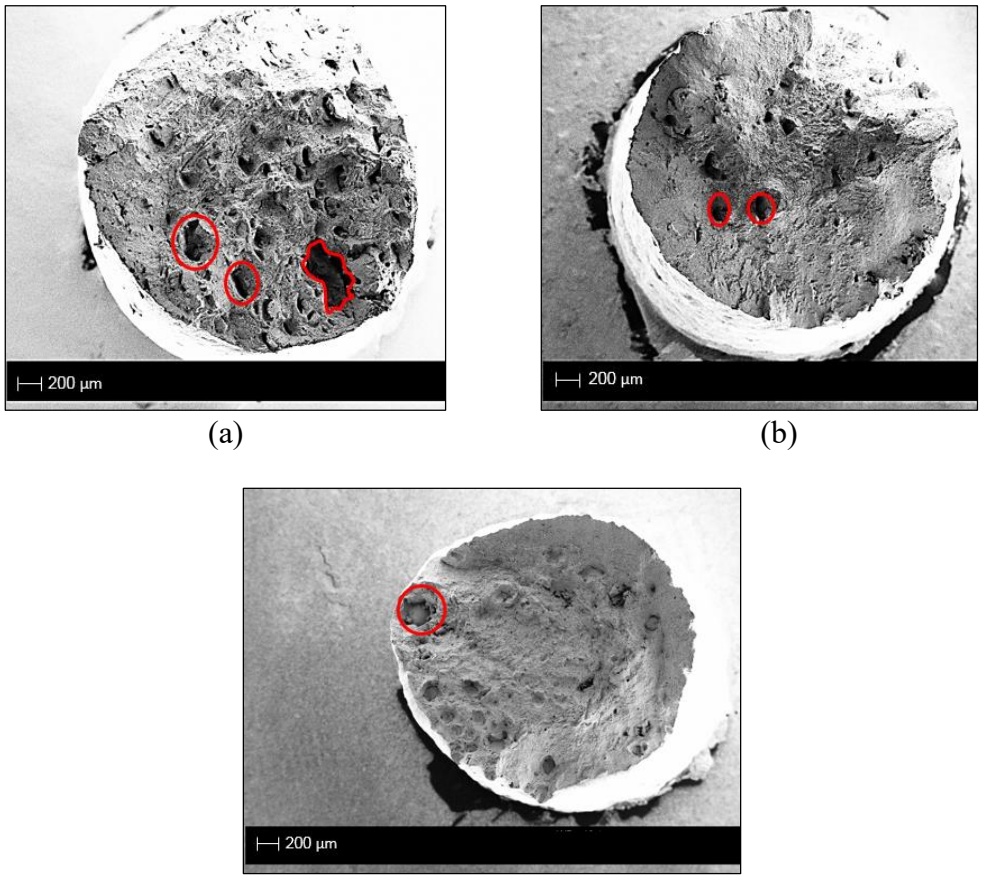

Figure 4. SEM images of overall fracture surfaces of L-PBF SS 316L specimens built in (a) horizontal, (b) diagonal, and (c) vertical directions subjected to monotonic tensile loading.

4. Fatigue Behavior

Fatigue failure is a common means for mechanical failure, as the majority of components and structures experience cyclic loading throughout their service life. AM induced defects can have significant effects on the fatigue life of AM components by causing stress concentration and providing localized plastic deformation [3]. In general, the fatigue life of a specimen can be categorized, based on the behavior of crack, into three stages; crack initiation, crack propagation, and the final failure. For AM parts, defects have been found to be the main factor responsible for crack initiation [3].

Strain-life (ε_a-N_f) curves, plotted using the experimental data obtained from the uniaxial strain-controlled fully-reversed (R_ε = -1) tests for the investigated L-PBF SS 316L specimens, are shown in Fig. 5. In general, among specimens built in three different directions, longer fatigue lives were observed for H specimens, while D specimens exhibited the shortest lives. Build orientation appeared to have less effect on the fatigue life at the highest strain amplitude of 0.4% (i.e. low cycle fatigue). For example, the average life of H specimens tested at 0.1% strain

amplitude is almost three times longer than D specimens, while the average lives of H and D specimens are comparable at 0.4% strain amplitude. This may be explained by less effects of the crack initiation stage and sensitivity to defects in the short life regime (i.e. higher strain amplitudes) [15].

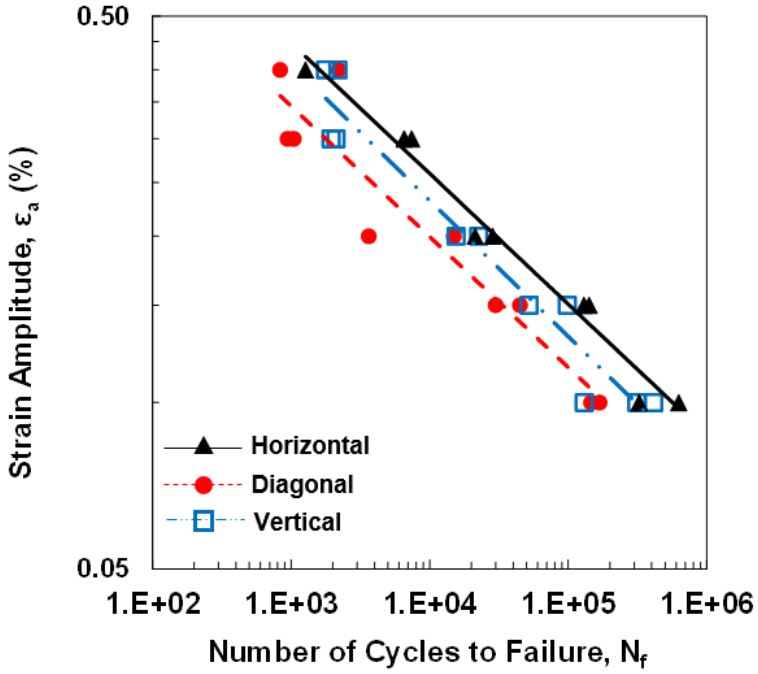

Figure 5. Strain-life curve obtained for L-PBF SS 316L specimens built in horizontal, diagonal, and vertical direction and subjected to uniaxial strain-controlled fully-reversed loading.

Fractography analysis was conducted to investigate factors responsible for crack initiation and the failure mechanisms inherent to fatigue specimens. Figures 6-8 display SEM images of fracture surface for the V, D, and H specimens, respectively, which were all subjected to 0.1% strain amplitude at 2.5 Hz. From these figures, three major types of defects were found to be responsible for crack initiation and failure in the L-PBF SS 316L specimens. These are LOF voids between subsequent layers in Fig. 6, inclusions formed due to partially melted powder in Fig. 7, and un-melted powder particles clustered together near voids in Fig. 8.

As displayed in Fig. 6, multiple LOF voids, which are typically oriented perpendicular to the build direction, were found to initiate fatigue cracks in the vertically built specimens. These deep LOF defects were observed at the specimen surface as denoted by red circles in Fig. 6(a). The crack coalescences from multiple initiation site, such as those shown in Fig. 6(a) are known to accelerate crack growth rate and may result in shorter fatigue life for V specimens. For the D specimen in Fig. 7, whose fatigue life is generally longer as compared to the V specimen when subjected to an identical cyclic loading condition, the crack was found to initiate from a single larger defect resulting from partially melted powder particles. This defect appeared to be relatively flat and located close to the surface of the specimen as shown in Fig. 7(b). For the horizontally

built specimen, it was observed that the crack initiated from un-melted powder particles clustered near and inside a LOF void, as illustrated in Fig. 8. This irregular shape LOF void was located slightly away from the surface. In addition, among the fracture surfaces for V, D, and H specimens shown in these figures, it can be noticed that the larger portion of the fracture surface of the H specimen seemed to be under the small crack growth regime as indicated by the smoother appearance, which could result in longer fatigue life for the H specimens. Furthermore, since LOF voids are generally oriented perpendicular to the loading direction in the V specimens and parallel to the loading direction in the H specimens, the effect of LOF voids may be more detrimental on the V specimens as compared to the H specimens [14]. It should be noted that, the SEM analysis presented in this study is only limited to the fatigue specimens subjected to 0.1% strain amplitude (i.e. long life regime). Hence, these observed defects in Figs. 6-8 are not necessarily distinctive for H, D, and V specimens. A comprehensive fractography analysis for all fatigue specimens is required to obtain the influence of build orientation on type and distribution of defects that cause fatigue failure.

The SEM images in Figs. 6-8 also indicated that the fatigue life of L-PBF SS 316L was sensitive not only to the types of defects, but also depended on the location and numbers of the defects. Nonetheless, fracture surface analysis alone cannot be utilized to fully explain the fatigue behavior observed in Fig. 5 (shortest fatigue life for D specimens and highest fatigue life for H specimens). Further studies of microstructural properties, such as grain size and grain orientation, may be required to accurately determine the effect of built orientation on the fatigue life of L-PBF specimens.

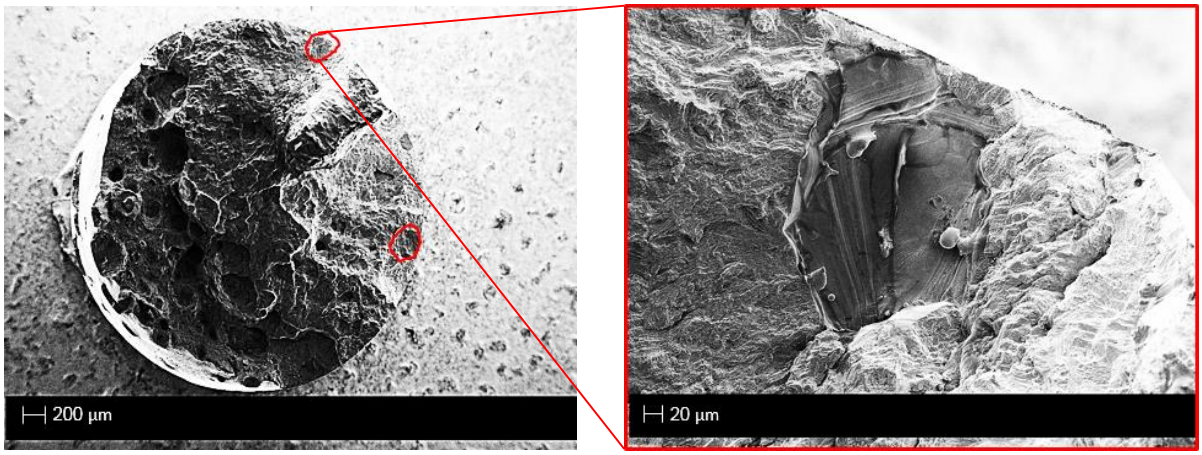

Figure 6. SEM images of a vertically built L-PBF SS 316L specimen subjected to fully-reversed uniaxial strain-controlled loading at 0.1% strain amplitude and 2.5 Hz showing (a) the overall fracture surface, and (b) void resulting from lack of fusion between subsequent layers that is responsible for the crack initiation.

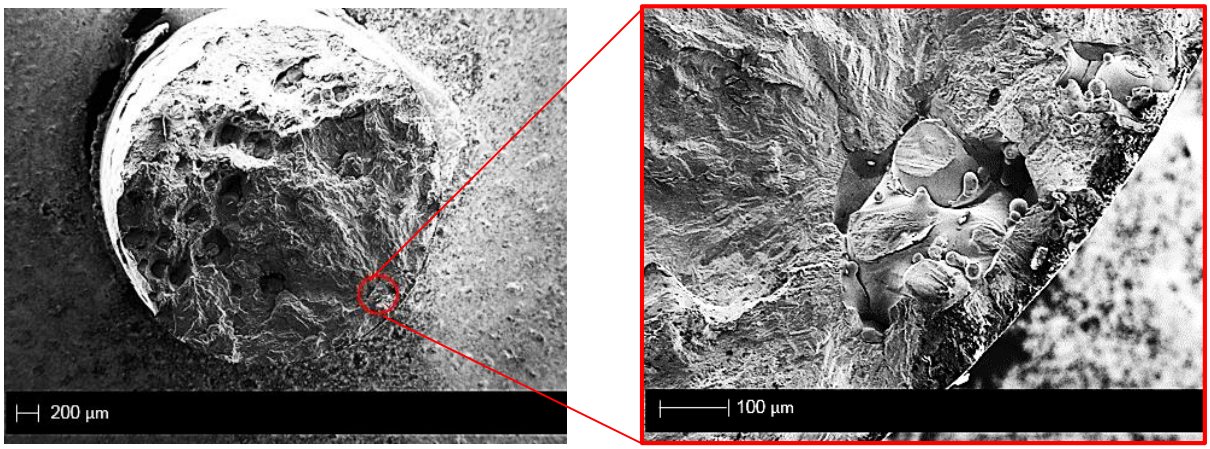

Figure 7. SEM images of a diagonally built L-PBF SS 316L specimen subjected to fully-reversed uniaxial strain-controlled loading at 0.1% strain amplitude and 2.5 Hz showing (a) the overall fracture surface, and (b) inclusion resulting from partially melted powder that is responsible for crack initiation.

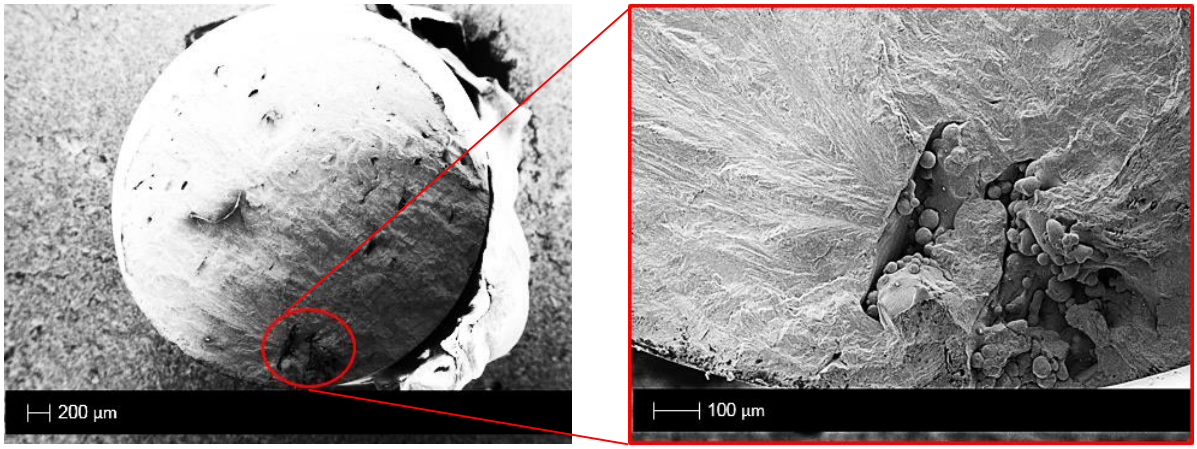

Figure 8. SEM images of a horizontally-built L-PBF SS 316L specimen subjected to fully-reversed uniaxial strain-controlled loading at 0.1% strain amplitude and 2.5 Hz showing (a) the overall fracture surface, and (b) inclusion resulting from lack of fusion and un-melted powder that is responsible for crack initiation.

Conclusions

In this study, SS 316L specimens, fabricated using the L-PBF process in three different build orientations (vertical, diagonal (i.e. 45° angle), and horizontal), were subjected to monotonic tensile and uniaxial strain-controlled fully-reversed (R_ε = -1) cyclic loading. Based on the experimental results, the following conclusions can be drawn:

1. All L-PBF SS 316L specimens, irrespective to build direction, exhibited higher yield and ultimate tensile stresses as compared to their wrought counterparts. In addition, when compared to those reported for wrought SS 316L, higher elongation to failure was obtained for vertically and diagonally built specimens.

2. Despites the fact that the D specimen possessed better tensile properties (i.e. yield stress, Young's modulus, and ultimate tensile stress) when compared to specimens oriented in vertical and horizontal directions, shorter fatigue lives were observed for the D specimens, while the H specimens exhibited higher fatigue resistance at low strain amplitudes (i.e. high cycle fatigue). Minimum effect of build orientation on fatigue life of L-PBF SS 316L specimens was found in the short life regime (i.e. higher strain amplitudes).

3. The significant effect of build orientation on the fatigue behavior of L-PBF SS 316L observed at high cycle fatigue can be attributed to greater effects of the crack initiation stage and sensitivity to defects.

4. Three major types of defects were observed to be responsible for the crack initiation and failure in L-PBF SS 316L specimens. These defects were voids formed due to the lack of fusion between the subsequent layers, inclusions formed due to partially melted powder particles, and un-melted powder particles clustered near a void.

5. Voids formed due to LOF between layers and their relative orientation to loading direction were observed to play an important role on the fatigue resistance of AM specimens.

Based on the results presented in this study, it has been shown that fracture surface analysis alone may not adequately explain the effects of build orientation on the tensile and fatigue behavior of L-PBF SS 316L specimens. Further studies on microstructural properties, such as grain orientation and size may be required. Additional work is also recommended to study the type and distribution of defects formed during fabrication resulting from different combination of process and design parameters, as significant effects of defects were observed on fatigue life of L-PBF SS 316L.

Acknowledgement

Research was partially sponsored by the Army Research Laboratory and was accomplished under Cooperative Agreement Number W911NF-15-2-0025. The views and conclusions contained in this document are those of the authors and should not be interpreted as representing the official policies, either expressed or implied, of the Army Research Laboratory or the U.S. Government. The U.S. Government is authorized to reproduce and distribute reprints for Government purposes notwithstanding any copyright notation herein. This manuscript was prepared while Nima Shamsaei and Scott Thompson were Assistant Professors at Mississippi State University.

References

[1] Thompson SM, Bian L, Shamsaei N, Yadollahi A. An overview of direct laser deposition for additive manufacturing; Part I: Transport phenomena, modeling and diagnostics. Addit Manuf 2015;8:36–62.

[2] Sterling AJ, Torries B, Shamsaei N, Thompson SM, Seely DW. Fatigue behavior and failure mechanisms of direct laser deposited Ti–6Al–4V. Mater Sci Eng A 2016;655:100–12.

[3] Shamsaei N, Yadollahi A, Bian L, Thompson SM. An overview of direct laser deposition for additive manufacturing; Part II: Mechanical behavior, process parameter optimization and control. Addit Manuf 2015;8:12–35.

[4] Yadollahi A, Shamsaei N, Thompson SM, Seely DW. Effects of process time interval and heat treatment on the mechanical and microstructural properties of direct laser deposited 316L stainless steel. Mater Sci Eng A 2015;644:171–83.

[5] Buddu RK, Chauhan N, Raole PM. Mechanical properties and microstructural investigations of TIG welded 40 mm and 60 mm thick SS 316L samples for fusion reactor vacuum vessel applications. Fusion Eng Des 2014;89:3149–58.

[6] Hermawan H, Ramdan D, Djuansjah JRP. Metals for biomedical applications, biomedical engineering - From theory to applications, Reza Fazel (Ed.). 2011.

[7] Triantafyllidis GK, Kazantzis AV, Karageorgiou KT. Premature fracture of a stainless steel 316L orthopaedic plate implant by alternative episodes of fatigue and cleavage decoherence. Eng Fail Anal 2007;14:1346–50.

[8] AlMangour B, Grzesiak D, Yang J-M. Rapid fabrication of bulk-form TiB2/316L stainless steel nanocomposites with novel reinforcement architecture and improved performance by selective laser melting. J Alloys Compd 2016;480–93.

[9] AlMangour B, Grzesiak D, Jenn-MingYang. Selective laser melting of TiC reinforced 316L stainless steel matrix nanocomposites: Influence of starting TiC particle size and volume content. Mater Des 2016;141–51.

[10] Spierings AB, Starr TL, Wegener K. Fatigue performance of additive manufactured metallic parts. Rapid Prototyp J 2013;19:88–94.

[11] ASTM E606-04, Standard Practice for Strain-Controlled Fatigue Testing, ASTM International, West Conshohocken, PA, 2004.

[12] Zhang B, Dembinski L, Coddet C. The study of the laser parameters and environment variables effect on mechanical properties of high compact parts elaborated by selective laser melting 316L powder. Mater Sci Eng A 2013;584:21–31.

[13] Yu J, Rombouts M, Maes G. Cracking behavior and mechanical properties of austenitic stainless steel parts produced by laser metal deposition. Mater Design 2013;45;228-235.

[14] Yadollahi A, Shamsaei N, Thompson SM, Elwany A, Bian L. Effects of building orientation and heat treatment on fatigue behavior of selective laser melted 17-4 PH stainless steel. Int J Fatigue 2016. doi:10.1016/j.ijfatigue.2016.03.014.

[15] Fatemi A, Fuchs HO, Stephens RI, Stephens RR. Metal fatigue in Engineering. 2001.